Investigations of the Watershield Effect on Blast Waves: One and Two-Dimensional Study

Minhyung Lee* and Young Sik Shin**

(*Received May 23, 1998*)

The object of this analysis is to investigate the mitigation effects of watershield on blast waves numerically. One application of current work is to resolve the design concerns for the ammunition storage facilities. To verify the numerical procedure using a multimaterial Eulerian finite element method, the results are compared with the available experimental data for detonation in a pressured tank, and the analytical predictions for air shocks. Features of the free-field detonation process are then studied from a series of one-dimensional simulations. The magnitude of peak pressure decreases and shock arrival time increases with increasing thickness of watershield. For design analysis, the case of two-dimensional axisymmetric geometry (a vertical right-circular cylinder) with a central charge is also considered. The full process including initial detonation, shock wave propagation and reflection from the outer rigid boundary is examined. For the explosives immersed in water, the magnitude of peak pressure becomes smaller than those in air tank without watershield. At later time period, the average gas pressure left in the air tank is about 20 bar.

Key Words: Watershield, Blast Wave Mitigation, Water Equation of State, Finite Element Method

Nomenclature

A,B	: Contstants in JWL equation
a_1,a_2,a_3	: Contstants in polynomial EOS
b_1,b_2,b_3	: Contstants in polynomial EOS
C_o	: Sound speed at undisturbed state
E	: Specific internal energy per unit mass
P	: Pressure
R_1,R_2	: Contstants in JWL equation
S_1,S_2,S_3	: Coefficients of the slope of U_s-u_p curve
t	: Initial explosive thickness
t_a	: Shock arrival time
U_s	: Shock velocity
u_p	: Fluid particle velocity
x_o	: The largest cell thickness
x_i	: The smallest cell thickness
w	: Watershield thickness
Z	: Scaled distance ($m/kg^{1/3}$)

Greek characters

γ	: Ratio of specific heats
η	: compression radio (ρ/ρ_o)
μ	: $\eta-1$
ρ	: density

* School of Mechanical and Aerospace Engineering Sejong University, Korea
** Department of Mechanical Engineering Naval Postgraduate School, USA

1. Introduction

Underwater explosion, blast waves in air and the consequent damage to nearby structures have been of great interest in both defense science and academic areas. Both state-of-the-art computational and experimental studies in these areas have been conducted by many researchers. However, the purpose of current work is to investigate the mitigation effects of water, which shields explosives, on the generation and propagation of blast waves. The test results demonstrated that water can reduce the peak gas pressure and the total impulse by as much as 90 percents, at

least for the range of test parameters (Keenan and Wager, 1992).

The shock waves produced by detonation propagate outward in all directions and aerosolize the water placed near the center of detonation. For this to occur, water medium delays the shock front and reduces the initial peak pressure, too. Furthermore, the aerosolized water expanding with detonation products absorbs detonation energy of the explosive. Typical heats of detonation for TNT is 980 cal/g. On the other hand, 539 calories are required to vaporize 1 gram water. Hence, water absorbing the significant detonation energy can actually reduce the total pressure impulse.

Recent large-scale experiments performed in the KLOTZ-Club tunnel in lvdalen (Hansson and Forsen, 1997), however, did not show any effect of the water mitigation due to other variations in the experiment setup. In order to exploit the potential advantages of watershield concept, spherically infinite one-dimensional domain and axisymmetric two-dimensional domain have been considered. The polynomial equation of state (EOS) of water which is based on the experimental shock Hugoniot data of published works are obtained and implemented into a non-linear Eulerian finite element program which solves the effects of shock physics.

Th equations of state for the materials considered in the study are described first. The numerical approach and verification are then addressed. The following two sections deal, respectively, with the numerical modeling and the calculation results. Final section is a summary of this study and suggests some directions for further research.

2. Equation of State

The pressure-volume-energy behavior of the detonation product gases of the TNT is modeled with the standard Jones-Wilkins-Lee (JWL) EOS and detonation velocity of 6930 m/s (Dobratz, 1981). The equation for pressure is:

$$P=A\left(1-\frac{\omega\eta}{R_1}\right)e^{-(R_1/\eta)}+B\left(1-\frac{\omega\eta}{R_1}\right)e^{-(R_2/\eta)}+\omega\eta\rho_o E \quad (1)$$

where the parameters for TNT are $A=3.712$ Mbar, $B=0.03231$ Mbar, $\omega=0.30$, $R_1=4.15$, $R_2=0.95$, $\eta=\rho/\rho_o$, ρ is the overall material density, $\rho_o=1630$ kg/m^3 (reference density), $E=4.29\times$ 103 KJ/kg (specific internal energy per unit mass). The Chapman-Jouguet pressure, P_{CJ}, is 0. 21 Mbar. Air is modeled as an ideal gas which uses a gamma law equation of state:

$$P=(\gamma-1)\frac{\rho}{\rho_o}E \quad (2)$$

where, $\gamma(=1.4)$ is the ratio of specific heats. The initial density of air, ρ_o, is 1 kg/m^3. To satisfy the standard atmosphere pressure of 1 bar, the initial internal energy, E, is 2.5 bar, which is determined from Eq. (2) and the value of γ at unperturbed stage. The unit of E are the unit of pressure.

Water is one of the most extensively studied materials under shock loading, i. e., at high pressures, densities, and temperatures (Mitchell & Nellis, 1982, Lalle, 1996). The shock compression data on water from experiments are analyzed using the Rankine-Hugoniot conservation equations which relate kinematic parameters to pressure, density, and internal energy in the shock state. There are two techniques for shock experiments on water. The first method is that the shock generated by plate impact compresses water sample. The second method is similar except for the explosive-driven shock. The range of shocked pressure in water is extensive. High explosives have been used to shock water to 100 GPa (Rice & Walsh, 1957). A two-stage light-gas gun has been used to achieve pressures up to 230 GPa (Mitchell & Nellis, 1982). Shock compression is also accompanied by an increase in temperature from 100℃ to several 10,000℃ for shocked water. Once shock Hugoniot data are obtained from the experiments, those can be implemented into a finite element program. The shock Hugoniot data is correlated by the cubic shock velocity-particle velocity equation,

$$\frac{U_s-C_o}{U_s}=S_1\left(\frac{U_s}{u_p}\right)+S_2\left(\frac{U_s}{u_p}\right)^2+S_3\left(\frac{U_s}{u_p}\right)^3 \quad (3)$$

where, C_o is the speed of sound at undisturbed state, S_1, S_2, and S_3 are the coefficients of the slope of the U_s-u_p curve. U_s and u_p are the

Table 1 Shock Hugoniot Parameters for water.

Model	C_o(km/s)	S_1	S_2	S_3	Rang(km/s)
Fusheng et al.	1.483	1.794	0	0	$u_p<3.5$
(1996)	2.404	1.337	0	0	$3.5<u_p<7.5$
HULL	1.483	1.75	0	0	
SNL	1.647	1.92	0	0	
Steinberg	1.480	2.56	-1.986	1.2268	
(1987)					
Lalle (1996)	1.483	1.75	0	0	$u_p<0.7$
	1.720	1.705	0	0	$0.7<u_p<2.03$
	2.510	1.316	0	0	$2.03<u_p<$

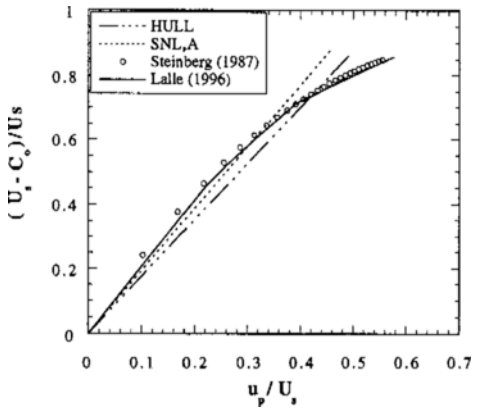

Fig. 1 Non-domensional shock velocity vs. fluid velocity.

shock wave and fluid particle velocities, respectively.

Most calculations showed that the water Hugoniot was the most important component in detonation study. Hence, five approximations from the shock Hugoniot experimental data were compared due to uncertainties in the data for water: The first model was provided by Fusheng et al. (1996) where two straight curves were fitted from experiments. They observed a phase transition at 25 GPa. This pressure corresponds to the particle velocity of 3.5 km/s. The phase transition was accompanied by a volume contraction. If an energy absorption process becomes significant, a change in slope should be observed. There is a linear data from the HULL code. A linear curve fit of data determined by Sandia National Laboratories (Weingarten, 1992) is also available. A curve fit of data using the nonlinear U_s-u_p provided by Steinberg (1987) is also widely used. Finally, the fifth model is the curve fit data provided by Lalle (1996). Lalle performed the shock loading experiments on water in the 0-30 GPa pressure range to determine shock Hugoniot. He obtained three linear curves with two kicks. The temperature for the first kick is 100℃. The parameters for these models are summarized in Table 1. Figure 1 shows the comparison of the non-dimensionalized values of shock wave velocity and fluid particle velocity for above parameters. It is observed that U_s-u_p curve can not be described by a straight line. Steinberg shock Hugoniot model which fits well to the experimental data of Lalle will be used for the current analysis.

The polynomial equation of state is used to model water. In this expression, the pressure is related to the relative volume and the specific internal energy by a cubic equation. In compression, the pressure is given by,

$$P=a_1\mu+a_2\mu^2+a_3\mu^3+(b_0+b_1\mu+b_2\mu^2)\rho_oE \quad (4)$$

and in tension, the pressure is given by,

$$P=a_1\mu+(b_0+b_1\mu)\rho_oE \quad (5)$$

where, $\mu=\eta-1$ and a_1, a_2, a_3, b_0, b_1, and b_2 are constants for water. Constants for these equations were determined by fitting the Mie-Gruneisen EOS to the polynomial EOS. That is, the constants in Eqs. (4) and (5) were determined, for both compression and expansion states, by matching terms in Eqs. (4) and (5) with the Steinberg shock Hugoniot data (Chisum & Shin, 1997). The values of the atmosphere condition EOS parameters determined by this procedure, appro-

priate for condensation values on the order of $\mu < 0.8$, are: $a_1 = 2.190 \times 10^9$ Pa, $a_2 = 9.224 \times 10^9$ Pa, $a_3 = 8.767 \times 10^9$ Pa, $b_0 = 0.4934$, $b_1 = 1.3937$, $b_2 = 0.0$, $\rho_0 = 1000$ kg/m^3.

The initial specific internal energy is 205.9 J/kg which is determined from Eq. (4) and the above parameters; it also represents the specific internal energy necessary to give the water an initial pressure equal to standard atmospheric pressure.

3. Numerical Modeling and Verification

The current problem including the explosion event, water shock, and blast waves propagation is modeled using the Eulerian finite element program MSC/DYTRAN (MacNeal-Schwendler Corporation, 1995). The multimaterial Eulerian scheme in this program allows up to nine different materials to be present in a given problem, and is likely suitable for the current study. The Eulerian scheme uses the basic conservation equations, in conjunction with the constitutive equation and the equation of state, to compute the solution in space.

To verify both the adequacy of the state equations and the numerical procedure for the simplest possible case, a comparison with the experimental data provided by Weingarten (1992) was conducted for a spherically symmetric one-dimensional problem. Four grams of Pentolite including detonator were placed near the center of pressurized tank (1150 psi), and a pressure signature was measured at a distance of 13.97 cm from the explosive center.

Non-rectangular hexahedron elements, whose top and bottom were parallel but whose sides had a slope of 0.1, were used to model the TNT and fluid medium. The mesh included 999 cells to a radius of 6 m. The first 0.00825 m to be filled with four gram TNT contains 25 equal length cells. The next 0.00825 m also contains 25 equal length cells. This region will be filled with water for the next problem. The cell size was then gradually increased by $x_o/x_i = 40$ until the mesh reached the outer boundary. x_o and x_i are the largest and smallest cell thicknesses, respectively. A flow boundary condition was specified in this outer boundary to satisfy the free-field condition. Pentolite is modeled with the standard JWL equation of state. The density of Pentolite is 1700 kg/m^3.

Figure 2 shows the pressure signatures from the numerical results and the corresponding experimental data measured at a distance of 13.97 cm. The first peak is the result of the initial shock wave, while the second pulse comes from bubble collapse. The good agreement in pressure signature shows that the current numerical scheme is

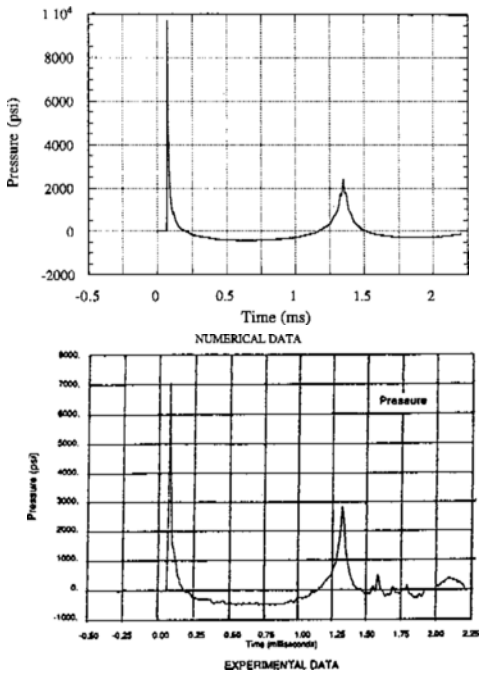

Fig. 2 Pressure signatures measured at 13.97 cm, numerical and experimental results.

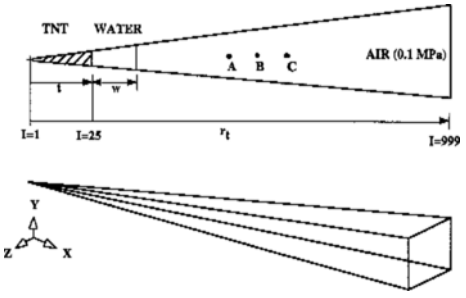

Fig. 3 Spherically symetric one-dimensinal model set-up.

capable of calculating the detonation processes.

4. One-Dimensional Study

4.1 Problem description

Figure 3 illustrates the one-dimensional free-field model setup. The same geometry and computational elements with the previous case are used to study the effects of water mitigation on blast waves. The features of air shock waves are also examined to provide a reference data and confidence in this numerical procedure. The results are verified using the analytical equations for air shocks. The main problem studied consists of the TNT charge of equal mass and contact watershield with ratio of the watershield thickness, w, to initial explosive radius, t, varying from values of 0 to 1. $w/t=0$ corresponds to air shocks without watershield.

The peak pressure are calculated at three locations, where scaled distance Z (distance away from the center with an energy release of one kilogram TNT in the standard atmosphere, m/kg $^{1/3}$) are 1, 1.5, and 2. The dimensions, including the calculation location, explosive and water thicknesses, used in the study are summarized in Table 2. The unit is (m, sec, kg), so the pressure is Pascal.

Table 2 Computational Parameters.

	Contact Watershield					
w/t	0	1/5	2/5	3/5	4/5	1
m_{water}/m_{TNT}	0	0.447	1.070	1.899	2.964	4.924
w (cm)	0	0.165	0.330	0.495	0.660	0.825
r_t (cm)	600					

4.2 Results

To explore air shocks, the detonation process in one atmosphere air medium is first considered. The pressure signatures calculated at A, B, C are displayed in Fig. 4, showing the typical blast waveforms. The pressure rises quickly to a peak pressure, P_{max} at t_a, and returns to the ambient pressure. The pressure then drops to a partial vacuum state. At close location (A), a secondary shock is also observed in this time period. Numerous repeated shocks of small amplitude at various times after the first shock indeed have been obser-

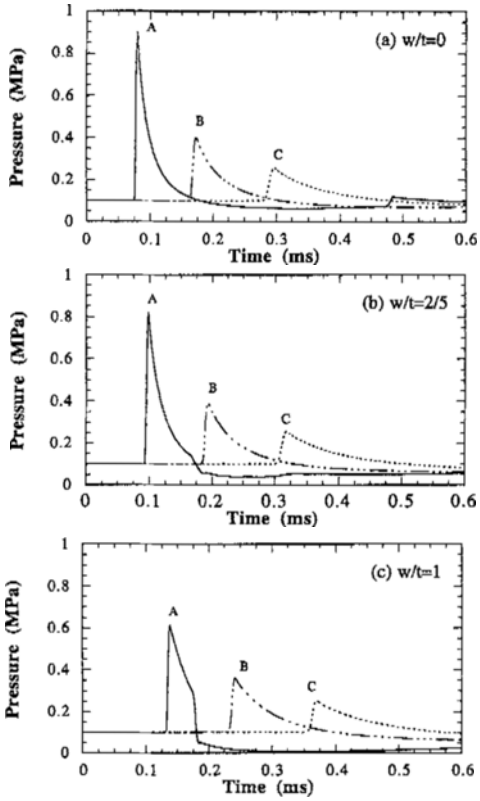

Fig. 4 Pressure signatures with contact watershield.

Table 3 Calculations and Analytic Results of overpressure in Air.

Location		t_a (ms/kg$^{1/3}$)	P^o ($\times 10^5$Pa)
A ($Z=1.0$m/kg$^{1/3}$)	CAL.	0.503	7.96
	Kinney (1985)	0.506	8.83
B ($Z=1.5$m/kg$^{1/3}$)	CAL.	1.087	3.00
	Kinney (1985)	1.098	3.96
C ($Z=2.0$m/kg$^{1/3}$)	CAL.	1.873	1.55
	Kinney (1985)	1.897	2.02

ved (Baker, 1973).

Analytic equations to predict characteristics of air shocks have been provided by Kinney and Graham (1985). Since shock velocity is uniquely related to overpressure ratio, the time required for that shock front to travel out to various distances can be also given. Table 3 summarizes the results for the magnitude of peak pressure and shock arrival time ($t_a/\mathrm{kg}^{1/3}$) from the numerical calculations and the above analytic equations. Good agreement in the shock arrival time can be obtained. The magnitudes of peak overpressure in each location are slightly underestimated compared to the results from the analytic equations.

The results dealing with air blast waves provide confidence in numerical modeling. Now, the effect of watershield in contact with the explosives on the generation of blast waves is examined. In Fig. 4, the calculated pressure signatures at A, B, C locations are also displayed for ratio of the watershield thickness to initial explosive radius of 0, 2/5, and 1. It is observed, as was anticipated, that the peak pressure continues to decrease with increasing the thickness of watershield and the shock arrival time is also delayed. This trend is realistic if we suppose the limiting case when the ratio of water thickness to explosive radius becones infinite. Then, this becomes the underwater explosion situation, and the pressure in air should drop to the atmosphere pressure.

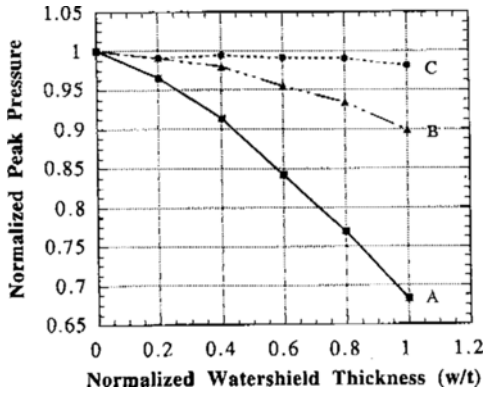

Fig. 5 Calculated peak pressures normalized by the peak pressure of no watershield.

Figure 5 shows the results for the magnitude of peak pressures normalized by the peak pressure without watershield. It is observed that the influence of watershield is most significant at close location (A), where the magnitude of peak pressure quickly starts to decrease and decays more than 30% for $w/t=1$. On the other hand, at far location (C), the magnitude remains almost constant and decays only 2% for $w/t=1$. The peak pressure at B location shows the intermediate characteristics. The initial shock waves are able to change water quickly into a mist of water droplets suspended in the atmosphere. By changing the water from a liquid state to a vapor state, huge amounts of energy released from the detonation is dissipated. Hence, this phenomenon results in a reduced total pressure impulse. Some test results demonstrate that water can reduce the peak gas pressure and total impulse by as much as 90 percents (Keenan and Wager, 1992).

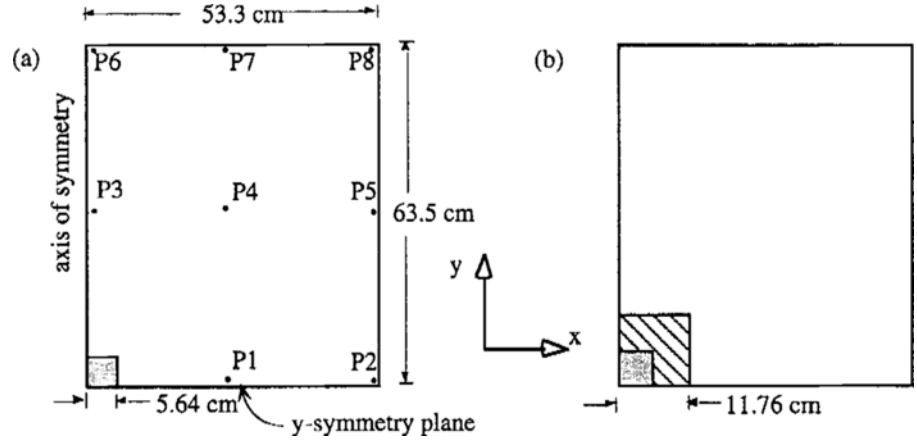

Fig. 6 Axisymmetric two-dimensional model setup.

5. Two-Dimensional Study

5.1 Problem description

Figure 6 illustrated the two-dimensional model setup. Four grams of TNT were placed near the center of a confined air tank (a rigid structure), and pressure signatures were measured at several locations in the tank. The second configuration (Fig. 6 (b)) includes 15.92 lb of water which is modeled as a cylinder of equal height and diameter shielding TNT. The pressure measurement locations are summarized in Table 4.

Due to the symmetry, only two-dimensional axisymmetry half plane is considered in the analysis. Non-rectangular hexahedron elements, whose top and bottom were parallel but whose sides had a slope of 0.1, were used to model the TNT and fluid medium. This was actually a extension of one-dimensional model to a two-dimensional wedge plane. The mesh included 3819 square cells (57×67). This cell dimension used in this analysis allowed the initial size of the two gram explosive to be modeled by approximately 36 cells (6×6) at the center.

If an exterior of an Eulerian mesh does not have a specific boundary condition, then, by default, it forms a barrier through which the material cannot flow. Materials are initialized with an uniform pressure of 1 atmosphere making use of an initial condition of Eulerian elements. The initial condition specifies the state of the material only at the beginning of the analysis.

Table 4 Location of Pressure time history.

Point	X (cm)	Y (cm)
P1	26	1
P2	52	1
P3	1	31
P4	26	31
P5	52	31
P6	1	62
P7	26	62
P8	52	62

Thereafter, the material state is determined by the calculation.

Although the key phenomena governing fluid-structure interaction (FSI) are the primary shock wave generation and reflection from the structure, simulations are carried out up to 5 msec in order to examine the average gas pressure at later stage. In this time period, several reflection waves are observed.

5.2 Results

In order to provide a base line data, the explosive was detonated without watershield. The same detonating explosive, but immersed in water, was next considered. The tank pressure is initially one atmosphere. A detonation wave travels through the explosive and propagates air medium. The shock wave propagation and the first reflection from the rigid boundary is observed until a time of 0.2 msec. Before the wave reaches outer boundary, momentum distribution in the air is spherically symmetric. The reflection waves from the side walls propagate back to the center and collide with the expanding detonation products. The expanding detonation products reach the outer boundary around 0.25 msec after the explosion. Because of the cylindrical geometry of the air tank and planar nature of the top and bottom walls, the reflection waves are quite different. The collision of the reflection waves from the side and top walls near the top corner produces a shock focusing which emanates from the corner. At later time, the waves are merging at the axis of symmetry again.

Pressure signatures calculated at several locations from the numerical simulations are shown in Fig. 7. After the first shock, several repeated shocks at various times have indeed been observed. These are caused by the successive reflection waves from the walls and shock focusing of those waves. Due to the shock focusing, for the case of no watershield, the magnitude of reflection waves are sometimes large than that of the initial detonation wave, as shown in the P1, P3, and P6 locations. At later time period, the air tank is pressurized to about 20 bar.

For the case of watershield, the magnitude of

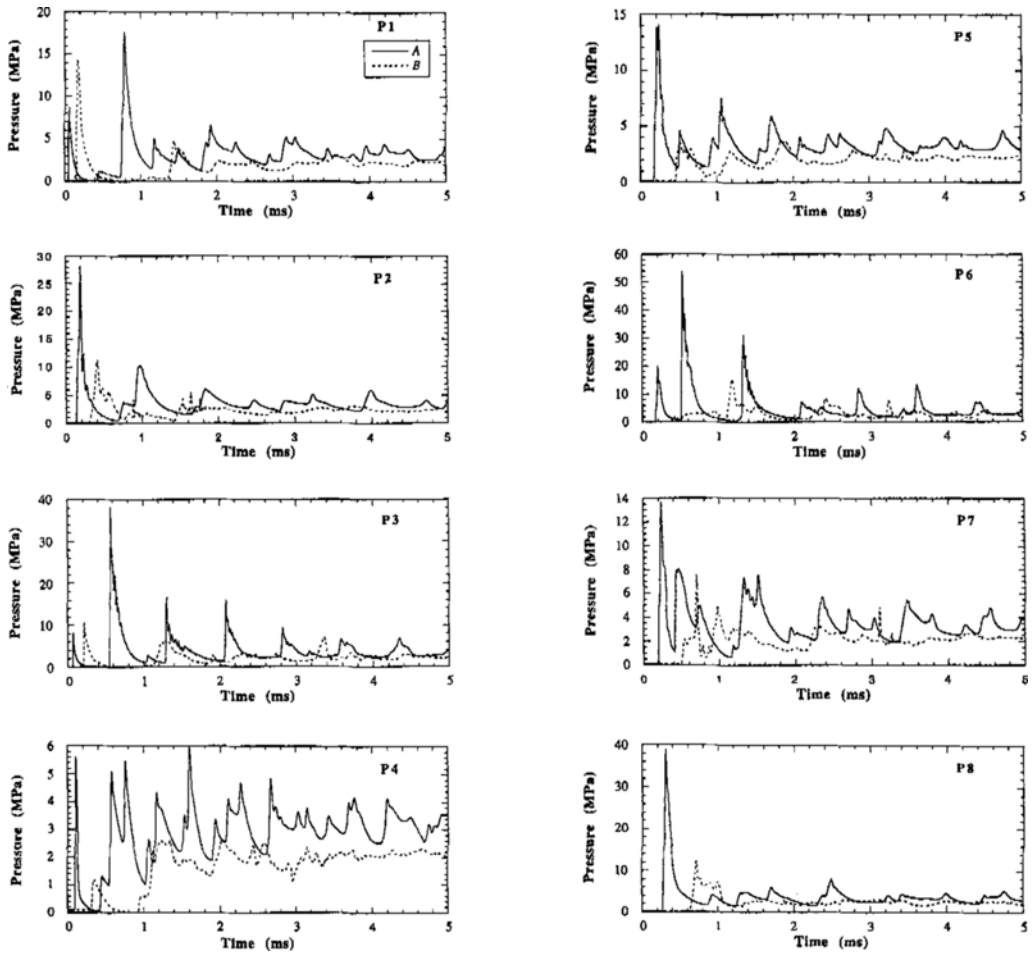

Fig. 7 Pressure signatures at P1 through P8 (A: without watershield, B: with watershield).

peak pressure diminishes compared to the case of the explosives in air medium only. At P3 location, an unique reflection wave from the water is observed at time 0.25 msec. This wave which follows the initial detonating wave can also be seen at P6 location. It is then smeared out due to the continued diffusion of shock front, but also due to the dissipative effects of shock interactions.

6. Conclusions

The effects of contact watershield on the generation and propagation of blast waves have been examined for one-dimensional free-field and two-dimensional axisymmetric cases using a multimaterial Eulerian finite element method. The computational simulation included modeling of the formation, propagation of water/air-shock waves, and reflections from the outer boundary, and shock focusing of the reflections waves in a confined air tank.

It has been shown that the water medium delays the shock front and reduces the magnitude of initial peak shock pressure. Later time period, the water mist expanding with detonation products absorbs detonation energy of the explosive, which can actually reduce the total pressure impulse. It has been also shown that the average gas pressure in the tank has become smaller than the case of no watershield. However, the reduction in the average gas pressure was not as much as 90 percents (test results by Keenan and Wager, 1992).

The fully coupled fluid-realistic structure inter-

action was not considered here for the purpose of understanding the physics involved. Study in these areas should be conducted in the future.

References

Baker, W. E., 1973, Explosions in Air. University of Texas Press, Austin USA.

Chisum, J. E. and Shin, Y. S., 1997, "Explosion Gas Bubbles Near Simple Boundaries," *Journal of Shock and Vibration*, Vol. 4 (1), pp. 11~25.

Dobratz, B. M., 1981, LLNL Explosive Handbook, UCRL-52997, Lawrence Livermore National Laboratory, Livermore, CA. USA.

Fusheng, L., Xianmong, C., Pansen, C., Juxing, C., Hua, T., Qingquan, G., and Fuqian, J., 1996, "Equation of State and Conductivity of Shocked Heavy Water," *Shock Compression of Condensed Matter*, pp. 57~60, American Institute of Physics.

Hansson, Hakan and Forsen Rickard, 1997, "Mitigation Effects of Water on Ground Shock: Large Scale Testing in Alvdalen," *FOA-R-97-311*, Defense

Research Establishment, Weapons and Protection Division, S-172 90, Stockholm, Sweden.

Keenan, W. A. and Wager, P. C., 1992, "Mitigation of Confined Explosion Effects by Placing Water in Proximity of Explosions," *Presented at the 25 th DoD Explosives Safety Seminar*, Anaheim, CA.

Kinney, G. F. and Graham, K. J., 1985, Explosive Shocks in Air. Second Edition, Springer-Verlag.

Lalle, R. C., 1996, "Dynamic Properties of Water: Sound Velocity and Refractive Index," *Shock Compression of Condensed Matter*, pp. 61~64, American Institute of Physics.

Mitchell, A. C. and Nellis, W. J., 1982, "Equation of State and Electrical Conductivity of Water and Ammonia Shocked to the 100 GPa (1Mbar) Pressure Range," *Journal of Chemistry and Physics*, Vol. 76 (12), 15 pp. 6273~6281.

MSC/DYTRAN User's Manual, 1994, MSC/DYTRAN Version 2.2, MacNeal-Schwendler Corporation, Los Angeles, CA. USA.

Rice, M. H. and Walsh, J. M., 1957, "Equation of State of Water to 250 Kilobars," *Journal of Chemistry and Physics*, Vol. 26, No. 4.

Steinberg, D. J., 1987, "Spherical Explosions and the Equation of State of Water," *Report UCID-20974, Lawrence Livermore National Laboratory*, Livermore, CA. USA.

Weingarten, L. I., Horstemeyer, M. F. & Trento, W. P., 1992, "Modeling Underwater Explosions with an Eulerian Code," *Proceedings of the 63rd Shock and Vibration Symposium*, pp. 269~277.